BBA - Molecular Basis of Disease 1865 (2019) 2267–2275

Contents lists available at ScienceDirect

BBA - Molecular Basis of Disease

journal homepage: www.elsevier.com/locate/bbadis

Asparaginyl endopeptidase induces endothelial permeability and tumor metastasis *via* downregulating zonula occludens protein ZO-1

Lichun Kang[a], Long Shen[a], Liqing Lu[a], Dekun Wang[a], Yong Zhao[a], Chuan'ai Chen[a], Lingfang Du[a], Junbo Gong[b], Yuying Zhang[a], Xue Mi[a], Rong Xiang[a], Mianzhi Zhang[c,*], Xiaoyue Tan[a,**]

[a] School of Medicine, State Key Laboratory of Medicinal Chemical Biology, Nankai University, Tianjin 300071, China
[b] Tianjin Key Laboratory of Modern Drug Delivery and High Efficiency, Tianjin University, Tianjin 300072, China
[c] Dongfang Hospital of Beijing University of Chinese Medicine, Beijing 100078, China

ARTICLE INFO

Keywords:
Asparaginyl endopeptidase
Endothelial permeability
Tumor metastasis
Zonula occludens-1

ABSTRACT

Zona occludens-1 (ZO-1) is a key component of tight junctions that govern the function of the endothelial barrier against tumor metastasis. Factors secreted by tumor cells contribute to the maintenance of tumor vascular networks. How tumor cell-derived protein signals regulate ZO-1 expression is unclear. Here, we explored the effect of tumor cell-secreted asparaginyl endopeptidase (AEP) on the permeability of endothelial cells in the tumor microenvironment. First, we confirmed the existence of AEP in conditioned medium (CM) from AEP-overexpressing MDA-MB-231 and 4T1 cells. Treatment with CM from AEP-overexpressing tumor cells increased the permeability and tumor cell transversal of an endothelial monolayer. Furthermore, CM from AEP-overexpressing tumor cells suppressed endothelial ZO-1 expression, as well as ZO-1-associated nucleic acid binding protein ZONAB. In addition, the level of phosphorylated STAT3 was increased by treatment with AEP-containing CM. A mutation of RGD or blocking integrin αvβ3 with antibody recovered the ZO-1 downregulation induced by AEP. *In vivo*, a lung metastatic mouse model showed increased endothelial permeability in the AEP-overexpressing group compared with the control group. An orthotopic tumor transplantation model was established using AEP-overexpression and compared with mice receiving control 4T1 cells. Compared with controls, overexpression of AEP increased lung metastatic foci and area, as well as vascular instability in primary tumors or lung metastatic sites. Moreover, endothelial ZO-1 was decreased in the AEP-overexpressing group. Taken together, our data show that tumor cell-derived AEP increases the permeability of endothelial barriers. Interactions between RGD and endothelial integrin αvβ3 mediate this effect by downregulating ZO-1.

1. Introduction

Metastasis has become the most life-threatening event in patients with breast cancer undergoing continuous radiotherapy, chemotherapy and surgical treatment [1]. Numerous studies have revealed that transversal of the endothelial barrier is the critical speed-limiting step during tumor cell metastasis [2]. Crosstalk between tumor cells and endothelial cells plays an important role in regulation of the endothelial barrier [3]. Identifying the pro-metastatic signal transduction mechanism mediating the response of endothelial cells to tumor cells will aid the development of novel treatment strategies against metastasis.

Endothelial tight junctions (TJs) are an integral part of the blood-tumor barrier and function to restrict tumor metastasis [4]. In addition to their function as a permeability barrier, TJs are also important signaling platforms and are involved in the manipulation of cellular stress responses [5,6]. As the first identified TJ protein, zonula occludens 1 (ZO-1) functions as a master regulator of endothelial TJs. After binding to different transmembrane proteins at the N-terminal and F-actin at the C-terminal, ZO-1 induces the remodeling of F-actin to determine the maintenance of TJ integrity in response to stress [7]. The activation of ZO-1/ZO-1-associated nucleic acid binding protein (ZONAB) and cooperative unit containing ZO-1 and JAM-A has been proven in various pathological contexts [8]. A recent study showed that ZO-1 regulated Rho GTPases by interacting with guanine nucleotide exchange factors and GTPase activating proteins [9]. The underlying mechanism involved in regulating ZO-1 in endothelial permeability is poorly understood.

Tumor cells secrete a variety of angiogenic factors including

* Correspondence to: M. Zhang, Dongfang Hospital of Beijing University of Chinese Medicine, 6 Fangxingyuan 1st Block, Fengtai District, Beijing 100078, China.
** Correspondence to: X. Tan, Department of Pathology, Medical School of Nankai University, 94 Weijin Road, Tianjin 300071, China.
E-mail addresses: zhangminying@nankai.edu.cn (M. Zhang), xiaoyuetan@nankai.edu.cn (X. Tan).

https://doi.org/10.1016/j.bbadis.2019.05.003
Received 21 January 2019; Received in revised form 22 April 2019; Accepted 7 May 2019
Available online 13 May 2019
0925-4439/

cytokines, miRNA and other protein signals that interact with endothelial surface receptors, contributing to the recruitment of endothelial cells and sustainment of tumor vascular networks [10–12]. Integrins are a group of heterodimeric cell surface receptors, and tumor cell-expressed integrins correlate with disease progress. Regarding endothelial cells, quiescent endothelium lacks integrin expression. However, tumor-associated vessels highly express integrin αvβ3, which has been implicated in the regulation of the key functions of endothelial barriers [13,14]. Integrin αvβ3 specifically recognizes the Arg-Gly-Asp (RGD)-containing sequence and a RGD-mimetic integrin αvβ3 inhibitor stimulated tumor growth and angiogenesis [15,16]. Interestingly, a conservative lysosomal proteinase asparaginyl endopeptidase (AEP) harbors an RGD motif [17]. In addition, the serum level of circulating AEP corelated positively with the malignancy of breast cancer [18], suggesting the potential role of AEP in regulating the permeability of endothelial barriers during tumor metastasis.

In this study, we explored the pro-metastatic effect of tumor cell-secreted AEP that induces the permeability of endothelial cells. Moreover, interactions between RGD in AEP and endothelial integrin αvβ3 lead to the downregulation of the TJ protein ZO-1 to promote tumor metastasis.

2. Material and methods

2.1. Cell lines and culture conditions

Human breast cancer cell MDA-MB-231, human umbilical vein endothelial cell HUVEC, mouse breast cancer cell 4T1 and mouse microvessel endothelial cell bEnd3 were obtained from the American Type Culture Collection (Manassas, VA, USA). MDA-MB-231 and bEnd3 cells were maintained in DMEM medium, whereas 4T1 and HUVECs were cultured in RPMI-1640 medium supplemented with 10% fetal bovine serum (FBS). To collect the conditioned medium, tumor cells were grown to 80% confluence and growth medium was replaced with basal medium for another 24 h. Medium from tumor cell cultures were harvested and centrifuged at 2000 ×*g* for 20 min to remove cell debris. Conditioned medium was collected for further experiments. To detect the expression of AEP in supernatant, 5 × SDS loading buffer was added into supernatant and boiled in 100 °C for 10 min. To imitate hypoxia, cobalt chloride $CoCl_2$ (100 μM) was added to tumor cells and incubated for 24 h [19]. To investigate the expression of AEP under hypoxia, MDA-MB-231 and 4T1 cells were incubated in normoxia or hypoxia (1% O2) for 24 h [20]. Cell lysates and conditioned medium were collected for further detection. AEP inhibitor RR-11a (500 nM) and RGD peptide were used to treat endothelial cells in various experiments.

2.2. Plasmids and lentivirus infection

Human and mouse legumain complementary DNA were amplified by reverse transcription PCR and then ligated into pLV-EF1α-MCS-IRES-Bsd (Biosettia, San Diego, CA, USA). The G119A mutant of legumain was cloned from the overexpression vector using primer pairs for G119A and finally ligated into the same vector. To establish legumain overexpressing cell lines, MDA-MB-231 and 4T1 cells were infected with pLV-EF1α-legumain-IRES-Bsd using a lentivirus transfection system (Biosettia). Linearized full-length human ZO-1 was cloned into a pcDNA™ 3.1 vector (Invitrogen, Carlsbad, CA, USA) with BamHI and *Xho*I (New England Biolabs, Ipswich, MA, USA). For ZO-1 overexpression, 5×10^5 HUVECs were transfected with 2.5 μg of plasmid by Lipofectamine 2000 (Invitrogen). An empty vector was used as a control.

2.3. Animal models

Six-to-eight weeks old female BALB/c mice were purchased from Beijing HFK Bio-Technology (Peking, China). Vascular permeability analysis *in vivo* was performed as previously described [12]. Lung microvasculature permeability was detected by the Rhodamine B-Dextran extravasation assay. Briefly, animals were intravenously administered with 1×10^6 4T1 control or stable AEP-overexpressing 4T1 cells resuspended in 100 μl of PBS *via* tail vein injection ($n = 5$). Then, 24 h after inoculation, mice were intravenously injected with Rhodamine B-Dextran 70,000 MW (Sigma, St. Louis, MO, USA) at 1 mg per 20 g body weight. Thirty min later, mice were sacrificed under euthanasia. Lungs were fixed in 4% paraformaldehyde for immunofluorescence staining. Cryosections of lungs (5 μm) were stained with an antibody against the vessel wall marker α-SMA (Sigma) and examined by fluorescence microscopy for Rhodamine B-Dextran extravasation. Images were captured with a FV1000 confocal microscope (Olympus, Tokyo, Japan). To establish a xenograft tumor model, 5×10^4 4T1 cells or stable AEP-overexpressing 4T1 cells resuspended in 100 μl of PBS were subcutaneously injected into the forth mammary fat pad ($n = 5$). Tumor growth curves were recorded every two days. Tumor volumes were calculated using the formula: $V = \pi \times [a^2 \times b]/6$, where a is the minor tumor axis and b is the major tumor axis. Mice were sacrificed at day 25 after injection. Primary tumors and lungs were separated for tissue sectioning and homogenate preparation. Experiments were performed in accordance with Nankai University Guidelines for Animal Experiments.

2.4. Western blotting

Cell extracts or tumor tissues were prepared by RIPA lysis buffer. Proteins were separated by SDS-PAGE, and target proteins were detected by the following antibodies: anti-legumain (Abcam, Cambridge, MA, USA), anti-β-actin (Santa Cruz Biotechnology, Santa Cruz, CA, USA), anti-ZO-1 (Invitrogen), anti-ICAM1 (Abcam), anti-VE-cadherin (Abcam), anti-HIF1α (Proteintech, Rosemont, IL, USA), anti-integrin αv (Abcam), anti-integrin β3 (Cell Signaling Technology, Danvers, MA, USA), anti-STAT3 (Santa Cruz), anti-p-STAT3 (Ser727) (Santa Cruz), anti-Akt (Cell Signaling Technology), anti-p-Akt (Ser473) (Cell Signaling Technology), anti-MEK1/2 (Cell Signaling Technology), anti-p-MEK1/2 (Ser217/221) (Cell Signaling Technology). Proteins were detected by chemiluminescence HRP substrate (Millipore, Billerica, MA, USA).

2.5. Adhesion assay

Endothelial cells (HUVEC or bEnd3) were seeded in a 96-well plate for 24 h. Tumor cells (MDA-MB-231 or 4T1) were resuspended in RPMI-1640 medium at 5×10^6 cells per ml. Then, 5 μl of calcein AM stock solution (Keygen, Nanjing, China) was added to a 1 ml tumor cell suspension and incubated at 37 °C for 30 min. Next, 100 μl of the calcein AM-labeled tumor cell suspension was added to a prepared 96-well plate containing endothelial cells and incubated at 37 °C for 2 h. The medium was removed, cells were washed twice with PBS buffer, and 200 μl of PBS was added to each well. Fluorescence was measured using a SpectraMax microplate reader (Molecular Devices, San Jose, CA, USA) at 494 nm excitation and 517 nm emission wavelengths. Images were captured with a FV1000 confocal microscope (Olympus).

2.6. Endothelial permeability and transendothelial migration (TEM) assay

Endothelial cells (HUVEC or bEnd3) were seeded in transwell inserts (8 μm pore size; Millipore) and grown to confluence. The cell monolayers were treated with different conditioned medium for 24 h. The permeability of pre-treated HUVEC monolayers was assessed by the fluorescence intensity of Rhodamine B-Dextran. Briefly, 150 μl Rhodamine B-Dextran (10 mg/ml) were added into the inserts for the indicated times (15, 30, or 60 min), which permeated through the treated cell monolayers into the wells below the inserts. The

Table 1
Primers for quantitative real-time polymerase chain reaction (qRT-PCR) assay.

Gene name(source)	Sequence (5′ → 3′)
AEP (*Homo sapiens*)	
Sense	GGACGTGGAAGATCTGACTAAA
Antisense	CTGGCTTTGCGTTTCATACC
ZO-1 (Homo sapiens)	
Sense	ATGGAGGAAACAGCTATATGGGA
Antisense	CCAAATCCAAATCCAGGAGCC
ZONAB (Homo sapiens)	
Sense	CTGCCATCAAGAAGAATAACCC
Antisense	CGTAACGACTCCCTTCCACA
ICAM1 (Homo sapiens)	
Sense	GCAAGAAGATAGCCAACCAA
Antisense	TGCCAGTTCCACCCGTTC
CDH5 (Homo sapiens)	
Sense	CCCTACCAGCCCAAAGTG
Antisense	CGGTCAAACTGCCCATAC
AEP (*Mus musculus*)	
Sense	AGAGGATGTGACTCCAGAGAA
Antisense	CCGTGGTCGGTGAAGTAAAT
ZO-1 (Mus musculus)	
Sense	GATGAGCGGGCTACCTTA
Antisense	TGGAGACTGCGTGGAA
ZONAB (Mus musculus)	
Sense	CGAGGGAACACAGCTCCAG
Antisense	CTGCCTTGGTCTCTTTGCCA

fluorescence intensities of medium in the wells were detected by a Spectra Max microplate reader (Molecular Devices) at 544 nm excitation and 590 nm emission wavelengths. To detect tumor cell transendothelial migration, calcein AM labeled MDA-MB-231 or 4T1 cells were added to the pre-treated endothelial cell monolayers with or without integrin αvβ3 antibody (Santa Cruz) (100 ng/ml) for 24 h. Cells on the upper inserts were scraped off and transwell filters were examined under a ZEISS AX10 microscope for invading calcein AM positive cells.

2.7. RNA extraction and real time-PCR

Total RNA was extracted with Trizol reagent (Invitrogen). cDNA was prepared by TransScript First-Strand cDNA Synthesis SuperMix (TransGen Biotech, Peking, China) using oligonucleotides (dT). Real-time PCR was performed using TransStart Top Green qPCR SuperMix (TransGen) in a CFXTM Real-Time Thermal cycler (Bio-Rad, Hercules, CA, USA). Primers used are listed in Table 1.

2.8. HE staining, immunohistochemical and immunofluorescence analysis

Tumor tissues and lungs from tumor models were fixed with paraformaldehyde, embedded in paraffin, and then sectioned. For HE staining, slides were stained with hematoxylin and eosin, dehydrated, and then mounted onto slides. For CD31 staining, slides were incubated at 4 °C overnight with anti-CD31 antibody (Abcam). After incubation with a biotinylated secondary antibody for 2 h and an avidin-peroxidase complex for 30 min, the sections were visualized with DAB and counterstained with hematoxylin. Images were captured by a CX31 microscope (Olympus). The vessel area was calculated using ImageJ software (National Institutes of Health, MD, USA). Tumor vessel tortuosity was measured by counting inflection points on CD31 immunostained sections and analyzing the frequency of inflection points as previously described [21]. For immunofluorescent staining, cells or tumor tissue sections were fixed with 4% paraformaldehyde for 20 min at room temperature and then blocked with 1% BSA for 1 h. Cells or sections were then incubated with primary antibodies against ZO-1 (Invitrogen) and α-SMA (Sigma) overnight at 4 °C. After washing with PBST, cells or sections were incubated with fluorescent labeled secondary antibodies for 1 h at room temperature. Nuclei were stained with 4′,6-diamidino-2-phenylindole (DAPI). Immunofluorescence images were obtained with a FV1000 confocal microscope (Olympus).

2.9. Statistical analysis

Significance was determined by two-tailed Student's *t*-test, and the values are presented as the mean ± S.E.M. All statistical analyses were performed using GraphPad Software (La Jolla, CA, USA). $p < 0.05$ was considered statistically significant.

3. Results

3.1. Tumor cells overexpress and secrete AEP under stress stimulation

Although the stress-induced overexpression of AEP has been described in tumor cells, the integrated evaluation of AEP expression patterns under diverse stress stimuli is unknown. We chose a human breast cancer cell line MDA-MB-231 and mouse breast cancer cell line 4T1 as models for studying the expression and secretion of AEP under diverse stress conditions *in vitro*. The expression of AEP mRNA was increased in cultured MDA-MB-231 or 4T1 cells after incubation with a hypoxia simulating reagent, $CoCl_2$ (Fig. 1A). The expression and secretion of AEP was increased in $CoCl_2$-treated MDA-MB-231 cells as indicated by western blotting of cell lysates and supernatants (Fig. 1B). Twenty-four hr of non-serum starvation also stimulated the expression of AEP in MDA-MB-231 cells, at the mRNA and protein levels (Fig. 1C). Hypoxia induced the upregulation of mature AEP in MDA-MB-231 and 4T1 cells (Fig. 1D). In stable AEP-overexpressing MDA-MB-231 and 4T1 cell lines, increased AEP expression was found in the supernatant (Fig. 1E & F). Similarly, the overexpression of AEP in the Her-2 enriched breast cancer cell line SK-BR-3 also increased the amount of AEP in the cell lysate and supernatant compared with control SK-BR-3 cells (Supplementary Fig. 1A). Together, these data indicate that the exogenous overexpression of AEP leads to the increase of AEP secretion.

3.2. Tumor cell-secreted AEP destroys endothelial cell adhesion and barrier function

To identify the effect of tumor-secreted AEP on the endothelial adhesion of tumor cells, an adhesion assay using tumor cells was performed on a HUVEC or bEnd3 endothelial monolayer. An increase of tumor cell adhesion was observed in AEP-overexpressing MDA-MB-231 or 4T1 cells compared with the controls (Fig. 2A & B). We next performed an *in vitro* permeability assay by measuring the transversion of Rhodamine B-Dextran through a HUVEC or bEnd3 endothelial monolayer. Treatment with CM from exogenous AEP-overexpressing tumor cells significantly increased the trans-endothelial permeability of Rhodamine-labeled Dextran (Fig. 2C & D and Supplementary Fig. 1B). The tumor cell transendothelial migration assay indicated that treatment of the endothelial monolayer with CM from exogenous AEP-overexpressing cancer cells significantly promoted the transendothelial migration of tumor cells compared with the controls (Fig. 2E & F). These data collectively suggest that the overexpression of AEP increases the adhesion of tumor cells and treatment with AEP-containing CM induces endothelial permeability.

3.3. Tumor cell-secreted AEP downregulates tight junction protein ZO-1

To explore the mechanism underlying the effect of AEP on endothelial permeability, we examined the expression of proteins associated with tight junctions after treatment with AEP-containing CM. ZO-1, a major component of tight junctions, but not ICAM1 or VE-cadherin, was significantly downregulated in HUVECs and bEnd3 cells after treatment with CM from AEP-overexpressing tumor cells (Fig. 3A-E and Supplementary Fig. 1C) compared with control tumor cell CM treatment groups. Other components of tight junctions including occludin (OCLN) and claudin5 (CLDN5) were detected by real-time PCR.

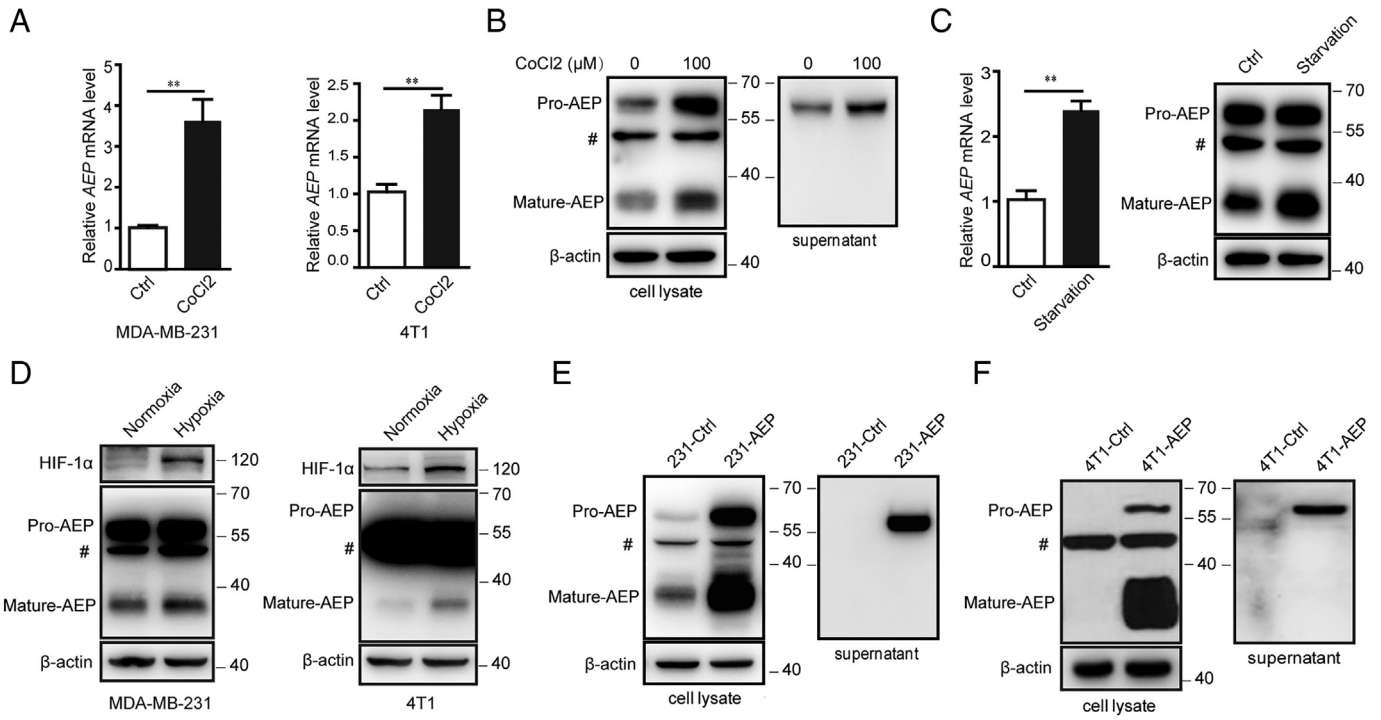

Fig. 1. Stress conditions induce the expression and secretion of AEP in breast cancer cells.
Cultured breast cancer cell lines MDA-MB-231 or 4T1 were treated with 100 μM cobaltous chloride for 24 h. (A) Statistics of real-time PCR assays for AEP expression. Data obtained from three independent experiments, ** $p < 0.01$. (B) Western blot assay of AEP in cell lysates (left panel) and supernatants (right panel). (C) Cultured MDA-MB-231 cells were treated with non-serum medium for 24 h. Statistical results of real-time PCR assay (left panel) and western blot assay (right panel) for AEP expression. Data obtained from three independent experiments, **$p < 0.01$. (D) MDA-MB-231 or 4T1 cells were cultured under conditions of normoxia or hypoxia. Western blot assay of HIF-1α and AEP in cell lysates. Stable AEP-overexpressing MDA-MB-231 (E) or 4T1 cells (F) were established. Western blot results of AEP in cell lysates (left panel) and supernatants (right panel). #: Nonspecific bands in images of western blot assay.

Compared with the 231 control CM group, the mRNA expression of OCLN remained unchanged while CLDN5 expression was increased in the AEP overexpressing CM group. Considering the increased transendothelial permeability by AEP-containing CM, we focused on the downregulated tight junction protein ZO-1 (data not shown). Structurally, ZO-1 binds to ZO-1-associated nucleic acid binding protein (ZONAB), a transcriptional and post-transcriptional regulator of gene expression. Significant inhibition of ZONAB mRNA was observed in HUVECs or bEnd3 following treatment with CM from AEP-overexpressing 231 or 4T1 cells (Fig. 3F & G). The transient overexpression of ZO-1 rescued the increase in endothelial permeability (Fig. 3H-J). Interestingly, treatment with CM from AEP-overexpressing 231 cells increased phosphorylated STAT3 at Ser727 in endothelial cells, and did not affect phosphorylation of Akt or MEK (Fig. 3K). Our data suggest that treatment with AEP-containing CM downregulates the tight junction protein ZO-1 as well as ZONAB in the endothelium *via* promoting phosphorylation of STAT3.

3.4. Integrin αvβ3-RGD mediates the pro-metastatic effect of AEP on the endothelial barrier

To assess whether the enzymatic activity of proteases or the RGD motif mediate the effect of AEP on endothelial ZO-1 and permeability, we measured ZO-1 expression following treatment with AEP-overexpressing CM with or without the enzyme inhibitor RR-11a. The administration of RR-11a had no effect on the suppression of ZO-1 expression by AEP-overexpressing CM (Fig. 4A). However, RGD peptide mimicked the effect of AEP-overexpressing CM on endothelial ZO-1 expression (Fig. 4B). Next, we constructed an AEP plasmid with an RGD motif replaced by RAD and established stable AEP^{G119A}-overexpressing MDA-MB-231 cells to confirm the role of RGD. The results showed that the mutation of RGD to RAD restored ZO-1 expression, which was suppressed by CM from AEP-overexpressing tumor cells (Fig. 4C-E). Consistent with the effect of the RGD mutation on ZO-1 expression, the mutation of RGD to RAD also rescued the increased endothelial permeability of dextran and tumor cells induced by the treatment of CM from AEP-overexpressing tumor cells (Fig. 4F & G). Next, we measured the expression of integrin αvβ3, a well-known interaction molecule related to RGD. The expression of integrin αvβ3 was increased after treatment with CM from AEP-overexpressing cancer cells compared with the control group (Fig. 4H). Moreover, the administration of neutralizing antibody against integrin αvβ3 significantly restored the suppressed ZO-1 expression as well as the increased transendothelial migration of tumor cells, compared with the IgG control group (Fig. 4I & J). These results indicate that interactions between the RGD motif in AEP and endothelial integrin αvβ3 mediate the effect of tumor cell-secreted AEP on ZO-1 and endothelial permeability.

3.5. Tumor-secreted AEP suppresses ZO-1 and induces pro-metastatic transendothelial permeability in vivo

To explore the effect of tumor cell-derived AEP on the endothelial barrier *in vivo*, we established a lung microvasculature permeability model by the intravenous injection of AEP-overexpressing or control 4T1 cells to mice, followed by the intravenous injection of Rhodamine B-Dextran (Fig. 5A). The results showed increased dextran penetration into lung tissues in the AEP-overexpressing group compared with the controls (Fig. 5B). An orthotopic xenograft tumor models using AEP-overexpressing or control 4T1 cells was set up to evaluate the effect of tumor cell-derived AEP on metastasis. There was no difference in tumor growth between the groups (Fig. 5C). However, a higher level of lung metastatic foci was observed in the AEP-overexpressing group compared with the control group (Fig. 5D). Suppressed ZO-1 expression in tumor homogenates and ZO-1 expression on $CD31^+$ vascular

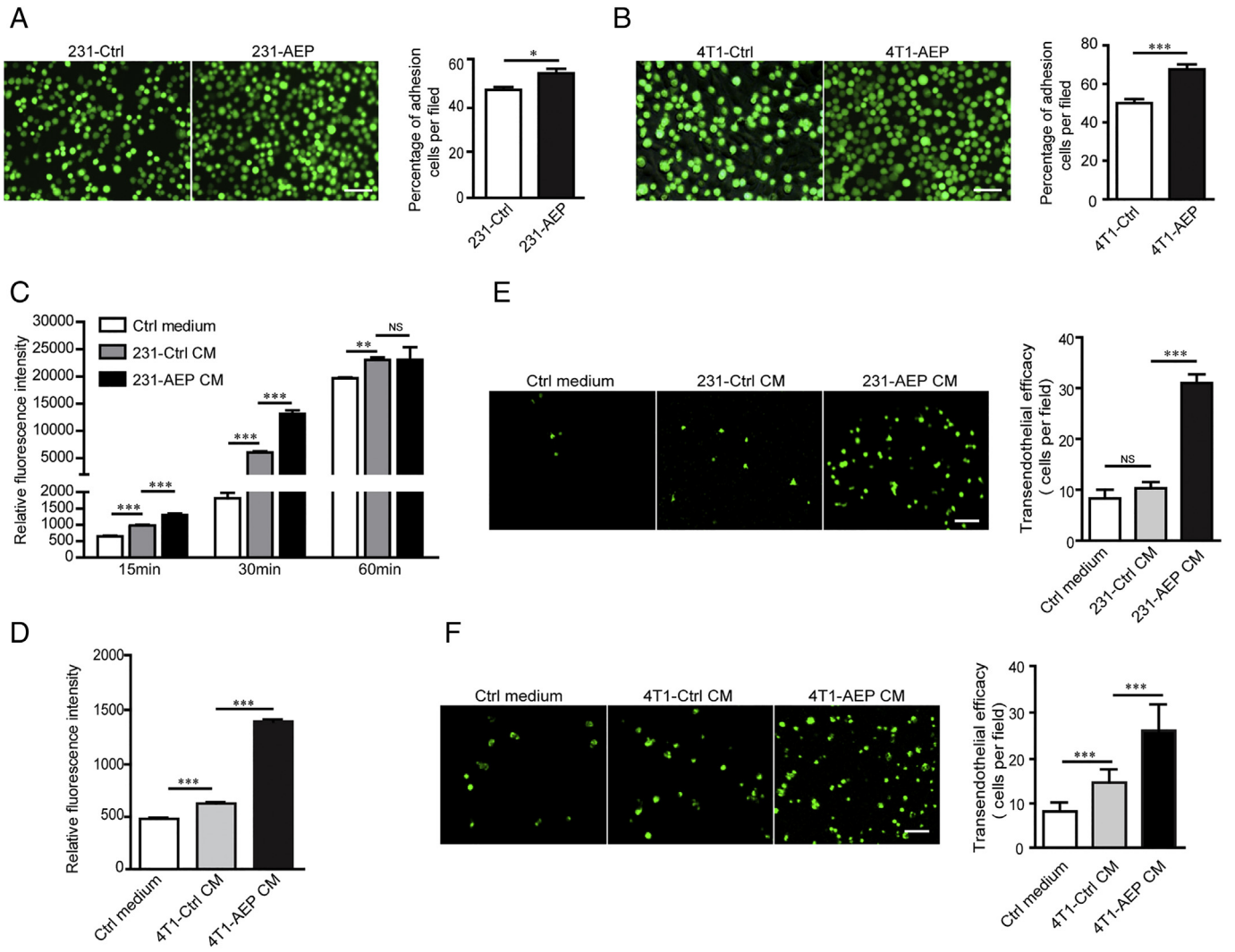

Fig. 2. Conditioned medium (CM) from AEP-overexpressing cancer cells promotes endothelial permeability.
Stable AEP-overexpressing MDA-MB-231 and 4T1 cell lines were established. Control construct-overexpressing cell lines were used. Representative images and statistical results of adhesion assay of AEP-overexpressing MDA-MB-231 (A) and 4T1 cells (B). Scale bar = 50 μm. Data obtained from three independent experiments, * $p < 0.05$, *** $p < 0.001$. The HUVEC monolayer was grown on 0.4-μm filters and treated with CM from stable AEP-overexpressing MDA-MB-231 (C) or 4T1 cells (D). Rhodamine B-Dextran was added to the top well at the beginning of the experiment for the indicated times. The absorbance at 590 nm at each time point was indicated. Data obtained from three independent experiments, ** $p < 0.01$, *** $p < 0.001$. HUVEC or bEnd3 monolayers were treated as described before. Calcein AM labeled MDA-MB-231 (E) or 4T1 cells (F) were added to the top well. Representative images and statistical results of the transendothelial migration of tumor cells are shown. Scale bar = 50 μm. Data obtained from three independent experiments, *** $p < 0.001$.

endothelial cells were observed in the AEP-overexpressing group compared with controls (Fig. 5E & F). Measurement of $CD31^+$ vascular number and density in the primary tumor tissue and lung metastatic foci showed imbalanced vascular status in the AEP-overexpressing group (Fig. 5G & H). Overall, our *in vivo* data suggest that tumor-secreted AEP suppresses endothelial ZO-1 and destroys vascular integrity, therefore promoting tumor metastasis.

4. Discussion

AEP belongs to clan CD and family C13 of cysteine proteases, which conserve recognition of the His^{148}-Gly-spacer-Ala-Cys^{189} motif [22]. Physiologically, mammalian legumain is most abundant in the kidney, testis and immune cells, while in the context of tumors, its overexpression and the unique distribution pattern of AEP were reported [23–25]. Tumor cells and tumor-associated macrophages were reported to overexpress AEP [26]. Although it is thought that AEP is present in acidic lysosomal environments, analysis of the AEP crystal structure and clarification of the mechanism of AEP degradation has provided support for its location outside the acidic endosome and lysosome, such as in the cytoplasm, nucleus and even on the cell surface [27]. In this study, we investigated the stimulated overexpression of AEP under different stress conditions, including serum-deprived starvation and hypoxia in tumor cells. AEP is synthesized as an inactive zymogen and its mature form requires the sequential removal of the C– and N-terminals. The zymogen form of AEP is stable at a neutral pH, whereas AEP activity is rapidly and irreversibly destroyed at a neutral pH because of its conformational unfolding [28]. Recent studies reported the oscillation of AEP between lysosomal and secretory pathways. An elaborate study revealed that oncogenic E3 ligase TRAF6 mediates the ubiquitination of proAEP by K63-linked polyubiquitin, and subsequently enhances the intracellular stability and secretion of AEP by forming a complex with HSP90α [18].

The functions of AEP are compelling considering its stress-stimulated expression and context-dependent distribution. The analysis of its crystal structure identified an enzymatically active endopeptidase domain that contributes to its protease activities [17]. Enzymatic activity of AEP outside the lysosome has also been widely reported under

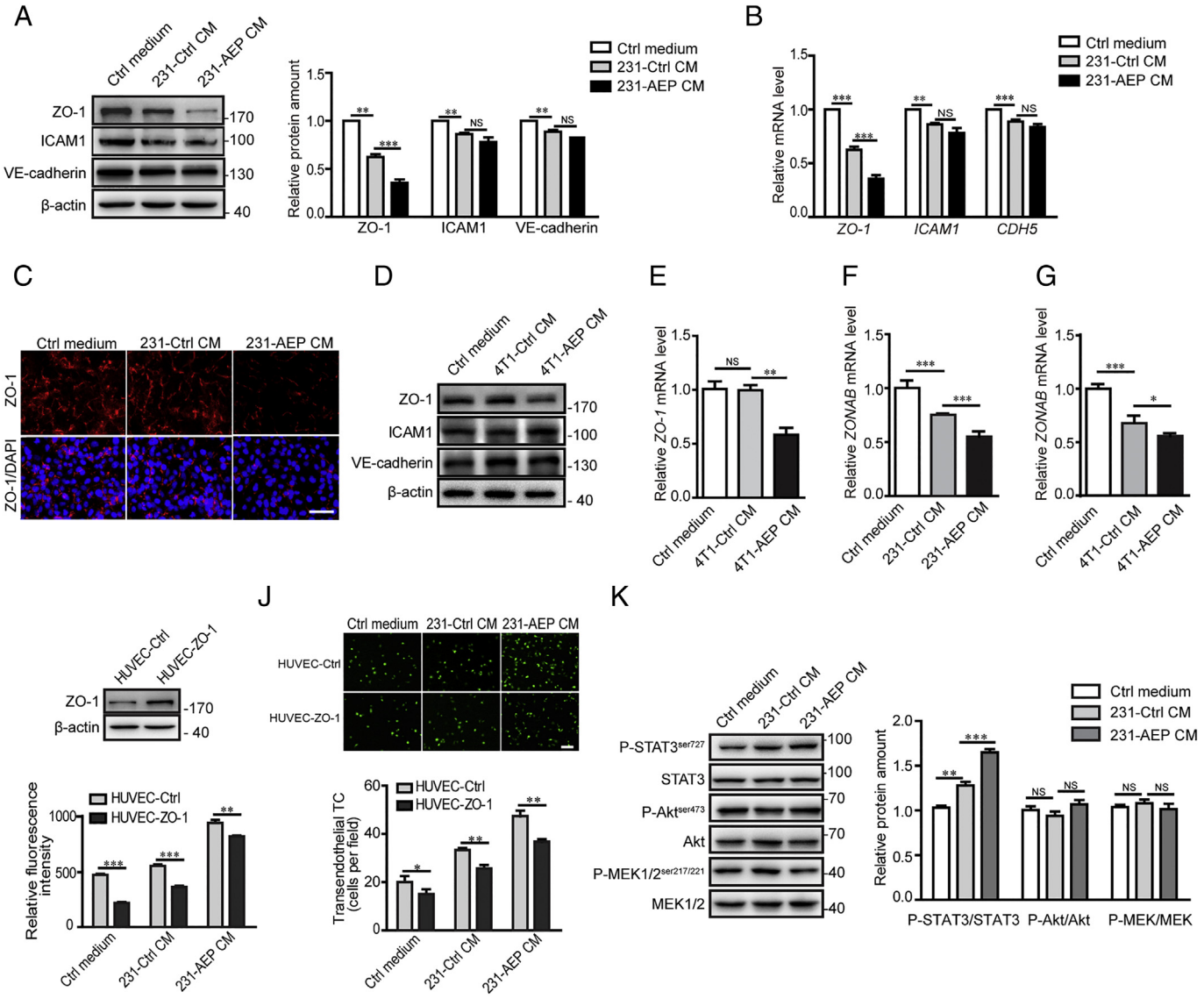

Fig. 3. Cancer cell-secreted AEP downregulates zonula occludens-1 (ZO-1) in endothelial cells.
HUVECs were treated with CM from stable AEP-overexpressing or control MDA-MB-231 cells. Non-serum culture medium was used as a blank control. (A) Western blot assay and statistics of HUVEC lysates using antibodies against ZO-1, ICAM1 and VE-cadherin. Data obtained from three independent experiments, ** $p < 0.01$, *** $p < 0.001$. (B) Real-time PCR assay of *ZO-1*, *ICAM1* and *CDH5 (VE-cadherin)* mRNA. Data obtained from three independent experiments, ** $p < 0.01$, *** $p < 0.001$. (C) Immunofluorescence staining of HUVECs using antibodies against ZO-1 (red). Nuclear staining was by DAPI (blue). Scale bar = 50 μm. bEnd3 cells were treated with CM from stable AEP-overexpressing or control 4T1 cells. Non-serum culture medium was used as a blank control. (D) Western blot assay of bEnd3 cell lysates using the antibodies against ZO-1, ICAM1 and VE-cadherin.
(E) Real-time PCR assay of *ZO-1*. Data obtained from three independent experiments, ** $p < 0.01$. (F & G) Real-time PCR assay of ZONAB mRNA. Data obtained from three independent experiments, * $p < 0.05$, ** $p < 0.01$, *** $p < 0.001$. (H) Western blot assay of HUVEC-Ctrl and HUVEC-ZO-1 cell lysates using antibodies against ZO-1. HUVEC-Ctrl or HUVEC-ZO-1 monolayers were treated as described before. (I) Rhodamine B-Dextran was added to the top well for 15 min at the beginning of the experiment. The absorbance at 590 nm is indicated. Data obtained from three independent experiments, ** $p < 0.01$, *** $p < 0.001$. (J) Calcein AM labeled MDA-MB-231 was added to the top well. Representative images and statistical results of the transendothelial migration of tumor cells were shown. Scale bar = 50 μm. Data obtained from three independent experiments, * $p < 0.05$, ** $p < 0.01$. (K) Western blot assay and statistical results of HUVEC lysates using antibodies against P-STAT^{ser727}, STAT3, P-Akt^{ser473}, Akt, P-MEK1/2$^{ser217/221}$, and MEK1/2. Data obtained from three independent experiments, ** $p < 0.01$, *** $p < 0.001$.

diverse pathologic conditions, such as excitoneurotoxicity and neurofibrillary pathology through its site-specific cleavage of the DNAse inhibitor SET and tau, respectively. In the tumor microenvironment, secreted AEP promotes tumor progression through degradation of the tumor matrix and in turn AEP protein levels may have prognostic implications in breast cancer patients. Interestingly, the catalytic domain harbors an RGD motif that is specific for interactions with integrin αvβ3. Our data showed that effects of tumor cell-secreted AEP on endothelial permeability are mediated by the interaction of AEP-bearing RGD with the endothelial integrin αvβ3 because the mutation of RGD to RAD or antibody against integrin αvβ3 partially rescued the effect of tumor-derived AEP on permeability of the endothelial barrier. Of note, it was reported that interactions with the RGD sequence led to allosteric changes, which resulted in different and opposite pharmacological effects on integrin activation [29]. In addition, whether the mechanism of AEP-bearing RGD binding with integrin is the same as for the RGD monomer requires solving its crystal structure.

The role of tumor cell-expressed integrin in tumor invasion,

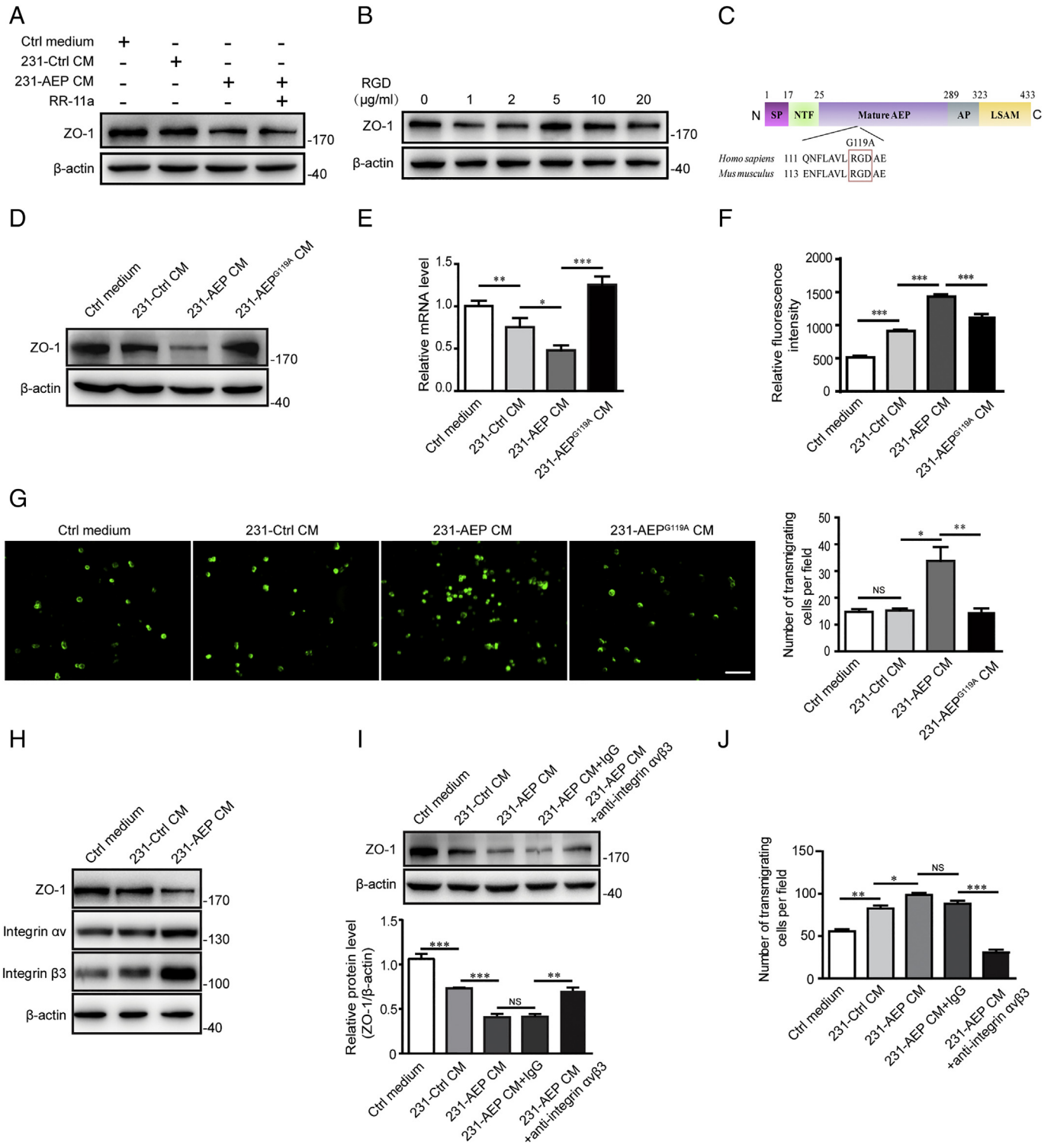

Fig. 4. Interaction of the RGD domain of AEP with integrin αvβ3 mediates the downregulation of ZO-1 in endothelial cells.
Cultured HUVECs were treated with conditioned medium from AEP-overexpressing MDA-MB-231 cells with or without enzymatic inhibitor of AEP, RR-11a. (A) Western blot assay of the HUVEC cell lysates using antibodies against ZO-1. (B) The indicated concentrations of RGD peptide were added into the culture medium of HUVECs for 24 h. Western blot assay of ZO-1. (C) Diagram of the G119A mutant location in the RGD motif. A stable overexpressing RGD mutant MDA-MB-231 cell line was constructed. HUVECs were treated with conditioned medium from RGD mutant or control 231 cells. (D) Western blot and (E) real-time PCR results of ZO-1. Data obtained from three independent experiments, * $p < 0.05$, ** $p < 0.01$, *** $p < 0.001$. (F) Results of the Rhodamine B-Dextran endothelial permeability assay. Data obtained from three independent experiments, ***$p < 0.001$. (G) Results of transendothelial migration assay. Left panel is a representative image and the right panel is the statistical results. Scale bar = 50 μm. Data obtained from three independent experiments, ** $p < 0.01$, * $p < 0.05$. Cultured HUVECs were treated with conditioned medium from stable AEP-overexpressing 231 or control cells. (H) Western blot detection of ZO-1, integrin αv and integrin β3 in HUVEC lysates. The HUVEC monolayer was treated with conditioned medium from AEP-overexpressing MDA-MB-231 cells with or without neutralizing antibody against integrin αvβ3. (I) Western blot assay and statistical results of ZO-1 expression. Data obtained from three independent experiments, ** $p < 0.01$, *** $p < 0.001$. (J) Statistical results of the transendothelial migration assay. Data obtained from three independent experiments, *$p < 0.05$, **$p < 0.01$, ***$p < 0.001$.

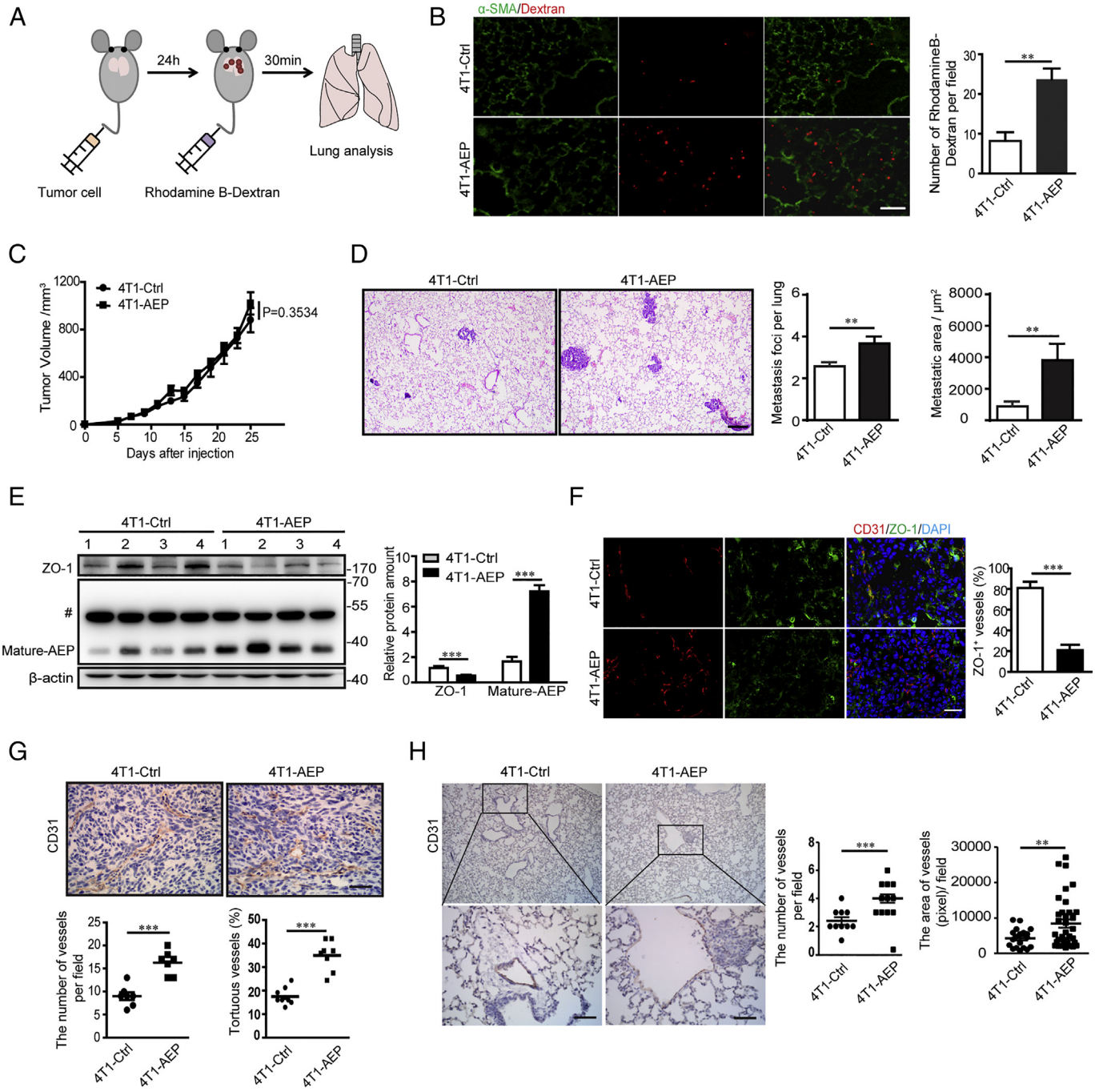

Fig. 5. Overexpression of AEP increases vascular permeability and tumor metastasis *in vivo*.
Rhodamine B-Dextran was intravenously injected 24 h after the intravenous injection of control 4T1 or stable AEP-overexpressing 4T1 cells. Lung vascular permeability analysis was performed. (A) Diagram of the experimental design. (B) Results of immunofluorescence staining using antibodies against α-SMA (green) and a fluorescence image of Rhodamine B (red). Left panel shows representative images and the right panel shows the statistics. Data obtained from ten different fields per group.** $p < 0.01$, scale bar = 50 μm. An orthotopic tumor model was set up using control 4T1 or stable AEP-overexpressing 4T1 cells. (C) Tumor growth curve. (D) Results of HE staining of lungs. Left panel shows a representative image and right panel is the statistical results for lung metastatic foci number and metastatic area. Data obtained from ten different fields per group.** $p < 0.01$, scale bar = 200 μm. (E) Western blot and statistics of ZO-1 and AEP in homogenized tumor tissue samples. $n = 4$, ***$p < 0.001$. (F) Representative images and statistical results of immunofluorescence staining for CD31 (red) and ZO-1(green). *** $p < 0.001$, scale bar = 50 μm. (G) Representative images (left panel) and statistical results (right panel) of immunohistochemistry for CD31 in primary tumor tissues and (H) lung metastatic foci. Each spot represents data from one tissue sample. *** $p < 0.001$, scale bar = 50 μm.

metastasis, proliferation, and survival has been studied extensively. Recent studies have shed new light on the role of endothelial integrin in mediating the responses of host cells in the microenvironment to tumor cells [30]. Endothelial cells in the tumor microenvironment highly express integrin αvβ3, which is available for exposure to environmental RGD sites. Their interactions then provide survival cues and/or signals for the pro-metastatic effect of endothelial cells. The integrin αvβ3 signaling pathway involving FAK and the S727 residue of the downstream STAT3 transcription factor has been reported. Phosphorylated STAT3 plays a non-transcriptional role in preserving the integrity of endothelial cells [31,32]. Consistently, tumor cell-secreted AEP stimulated the phosphorylation of STAT3 while mutations of RGD to RAD

abrogated this effect (data not shown), indicating that the interaction between RGD and integrin αvβ3 promotes activity of the STAT3 signaling pathway.

It is well-known that an important step in the formation of cancer metastases is the interaction and penetration of the vascular endothelium by dissociated cancer cells. Tight junctions (TJ) govern the permeability of endothelial cells and function as a barrier to prevent cancer metastasis. ZO-1 anchors the transmembrane proteins of TJ and binds the raft of TJ molecules together as a scaffold. In breast cancer, ZO-1 was decreased in poorly differentiated tumors and correlated with increasing Grade and TNM status. Our study identified the effect of tumor cell-secreted AEP on the downregulation of ZO-1 in the endothelial layer, which disrupted monolayer barriers allowing the traversal of cancer cells. The mechanism underlying the effect of ZO-1 downregulation on the disruption of endothelial barrier is still unknown. A previous study showed that ZO-1 functions as a major cytoskeletal organizer in EC, mediating the effect of tight junctions on the adherent junctions. RhoA regulates actin-myosin contractility, TJ assembly, and endothelial capillary formation through phosphorylation of the regulatory myosin light chain by Rho-associated protein kinase. In addition, ZO-1 interacts with the Y-box transcription factor ZONAB, which is a member of the family of DNA-binding proteins that regulate the expressions of genes involved in proliferation. Interactions of ZONAB with ZO-1 are critical for the tight junction-associated signal transduction pathway regulation of phenotype changes [33]. Understanding how these pathways are regulated and intersect with each other may help provide new mechanistic insights into metastasis.

In summary, our study uncovered a novel mechanism of AEP regulation and its role in breast cancer metastasis. Therefore, AEP might be of prognostic value and a potential therapeutic target for breast cancer. These findings provide a new mechanistic basis for targeting tumor-derived legumain and RGD-integrin αvβ3 interactions to prevent metastatic disease.

Supplementary data to this article can be found online at https://doi.org/10.1016/j.bbadis.2019.05.003.

Transparency document

The Transparency document associated this article can be found, in online version.

Declaration of Competing Interest

The authors have no conflicts of interest to declare.

Acknowledgments

We thank Edanz Group China (www.liwenbianji.cn/ac), for editing the English text of a draft of this manuscript. This work was supported by the National Natural Science Foundation of China (No. 81872254, to X.T.), the National Natural Science Foundation of China (No. 81502297, to X.M.), and the Tianjin National Natural Science Foundation of China (No. 16JCYBJC26300, to X.T.).

References

[1] A.W. Lambert, D.R. Pattabiraman, R.A. Weinberg, Emerging biological principles of metastasis, Cell 168 (2017) 670–691.
[2] B. Strilic, S. Offermanns, Intravascular survival and extravasation of tumor cells, Cancer Cell 32 (2017) 282–293.
[3] N. Reymond, B.B. d'Agua, A.J. Ridley, Crossing the endothelial barrier during metastasis, Nat. Rev. Cancer 13 (2013) 858–870.
[4] Z. Zeng, Y. Li, Y. Pan, X. Lan, F. Song, J. Sun, K. Zhou, X. Liu, X. Ren, F. Wang, J. Hu, X. Zhu, W. Yang, W. Liao, G. Li, Y. Ding, L. Liang, Cancer-derived exosomal miR-25-3p promotes pre-metastatic niche formation by inducing vascular permeability and angiogenesis, Nat. Commun. 9 (2018) 5395.
[5] C. Zihni, C. Mills, K. Matter, M.S. Balda, Tight junctions: from simple barriers to multifunctional molecular gates, Nat. Rev. Mol. Cell Biol. 17 (2016) 564–580.
[6] T.A. Martin, W.G. Jiang, Loss of tight junction barrier function and its role in cancer metastasis, Biochim. Biophys. Acta 1788 (2009) 872–891.
[7] A.S. Fanning, J.M. Anderson, Zonula occludens-1 and -2 are cytosolic scaffolds that regulate the assembly of cellular junctions, Annals of the New York Academy of Sciences, 1165 (2009) 113–120.
[8] O. Tornavaca, M. Chia, N. Dufton, L.O. Almagro, D.E. Conway, A.M. Randi, M.A. Schwartz, K. Matter, M.S. Balda, ZO-1 controls endothelial adherens junctions, cell-cell tension, angiogenesis, and barrier formation, J. Cell Biol. 208 (2015) 821–838.
[9] S. Citi, D. Spadaro, Y. Schneider, J. Stutz, P. Pulimeno, Regulation of small GTPases at epithelial cell-cell junctions, Mol. Membr. Biol. 28 (2011) 427–444.
[10] C. Huang, N. Li, Z. Li, A. Chang, Y. Chen, T. Zhao, Y. Li, X. Wang, W. Zhang, Z. Wang, L. Luo, J. Shi, S. Yang, H. Ren, J. Hao, Tumour-derived interleukin 35 promotes pancreatic ductal adenocarcinoma cell extravasation and metastasis by inducing ICAM1 expression, Nat. Commun. 8 (2017) 14035.
[11] W. Zhou, M.Y. Fong, Y. Min, G. Somlo, L. Liu, M.R. Palomares, Y. Yu, A. Chow, S.T. O'Connor, A.R. Chin, Y. Yen, Y. Wang, E.G. Marcusson, P. Chu, J. Wu, X. Wu, A.X. Li, Z. Li, H. Gao, X. Ren, M.P. Boldin, P.C. Lin, S.E. Wang, Cancer-secreted miR-105 destroys vascular endothelial barriers to promote metastasis, Cancer Cell 25 (2014) 501–515.
[12] M. Tichet, V. Prod'Homme, N. Fenouille, D. Ambrosetti, A. Mallavialle, M. Cerezo, M. Ohanna, S. Audebert, S. Rocchi, D. Giacchero, F. Boukari, M. Allegra, J.C. Chambard, J.P. Lacour, J.F. Michiels, J.P. Borg, M. Deckert, S. Tartare-Deckert, Tumour-derived SPARC drives vascular permeability and extravasation through endothelial VCAM1 signalling to promote metastasis, Nat. Commun. 6 (2015) 6993.
[13] Z. Liao, A. Kasirer-Friede, S.J. Shattil, Optogenetic interrogation of integrin alphaVbeta3 function in endothelial cells, J. Cell Sci. 130 (2017) 3532–3541.
[14] J.S. Desgrosellier, D.A. Cheresh, Integrins in cancer: biological implications and therapeutic opportunities, Nat. Rev. Cancer 10 (2010) 9–22.
[15] Y. Cheng, Y. Ji, RGD-modified polymer and liposome nanovehicles: recent research progress for drug delivery in cancer therapeutics, Eur. J. Pharm. Sci. 128 (2019) 8–17.
[16] Y. Liu, K.M. Bajjuri, C. Liu, S.C. Sinha, Targeting cell surface alpha(v)beta(3) integrin increases therapeutic efficacies of a legumain protease-activated auristatin prodrug, Mol. Pharm. 9 (2012) 168–175.
[17] E. Dall, H. Brandstetter, Mechanistic and structural studies on legumain explain its zymogenicity, distinct activation pathways, and regulation, Proc. Natl. Acad. Sci. U. S. A. 110 (2013) 10940–10945.
[18] Y. Lin, Y. Qiu, C. Xu, Q. Liu, B. Peng, G.F. Kaufmann, X. Chen, B. Lan, C. Wei, D. Lu, Y. Zhang, Y. Guo, Z. Lu, B. Jiang, T.S. Edgington, F. Guo, Functional role of asparaginyl endopeptidase ubiquitination by TRAF6 in tumor invasion and metastasis, J. Natl. Cancer Inst. 106 (2014) dju012.
[19] Y. Yuan, G. Hilliard, T. Ferguson, D.E. Millhorn, Cobalt inhibits the interaction between hypoxia-inducible factor-alpha and von Hippel-Lindau protein by direct binding to hypoxia-inducible factor-alpha, J. Biol. Chem. 278 (2003) 15911–15916.
[20] Y.L. Hsu, J.Y. Hung, W.A. Chang, Y.S. Lin, Y.C. Pan, P.H. Tsai, C.Y. Wu, P.L. Kuo, Hypoxic lung cancer-secreted exosomal miR-23a increased angiogenesis and vascular permeability by targeting prolyl hydroxylase and tight junction protein ZO-1, Oncogene 36 (2017) 4929–4942.
[21] E. Bullitt, G. Gerig, S.M. Pizer, W. Lin, S.R. Aylward, Measuring tortuosity of the intracerebral vasculature from MRA images, IEEE Trans. Med. Imaging 22 (2003) 1163–1171.
[22] E. Dall, H. Brandstetter, Structure and function of legumain in health and disease, Biochimie 122 (2016) 126–150.
[23] Y. Ohno, J. Nakashima, M. Izumi, M. Ohori, T. Hashimoto, M. Tachibana, Association of legumain expression pattern with prostate cancer invasiveness and aggressiveness, World J. Urol. 31 (2013) 359–364.
[24] L. Wang, S. Chen, M. Zhang, N. Li, Y. Chen, W. Su, Y. Liu, D. Lu, S. Li, Y. Yang, Z. Li, D. Stupack, P. Qu, H. Hu, R. Xiang, Legumain: a biomarker for diagnosis and prognosis of human ovarian cancer, J. Cell. Biochem. 113 (2012) 2679–2686.
[25] Q. Yan, W.B. Yuan, X. Sun, M.J. Zhang, F. Cen, S.Y. Zhou, W.B. Wu, Y.C. Xu, L.H. Tong, Z.H. Ma, Asparaginyl endopeptidase enhances pancreatic ductal adenocarcinoma cell invasion in an exosome-dependent manner and correlates with poor prognosis, Int. J. Oncol. 52 (2018) 1651–1660.
[26] Z. Liu, M. Xiong, J. Gong, Y. Zhang, N. Bai, Y. Luo, L. Li, Y. Wei, Y. Liu, X. Tan, R. Xiang, Legumain protease-activated TAT-liposome cargo for targeting tumours and their microenvironment, Nat. Commun. 5 (2014) 4280.
[27] M.H. Haugen, H.T. Johansen, S.J. Pettersen, R. Solberg, K. Brix, K. Flatmark, G.M. Maelandsmo, Nuclear legumain activity in colorectal cancer, PLoS One 8 (2013) e52980.
[28] L. Zhao, T. Hua, C. Crowley, H. Ru, X. Ni, N. Shaw, L. Jiao, W. Ding, L. Qu, L.W. Hung, W. Huang, L. Liu, K. Ye, S. Ouyang, G. Cheng, Z.J. Liu, Structural analysis of asparaginyl endopeptidase reveals the activation mechanism and a reversible intermediate maturation stage, Cell Res. 24 (2014) 344–358.
[29] L.M. Miller, J.M. Pritchard, S.J.F. Macdonald, C. Jamieson, A.J.B. Watson, Emergence of small-molecule non-RGD-mimetic inhibitors for RGD integrins, J. Med. Chem. 60 (2017) 3241–3251.
[30] G. Sokeland, U. Schumacher, The functional role of integrins during intra- and extravasation within the metastatic cascade, Mol. Cancer 18 (2019) 12.
[31] N.P. Visavadiya, M.P. Keasey, V. Razskazovskiy, K. Banerjee, C. Jia, C. Lovins, G.L. Wright, T. Hagg, Integrin-FAK signaling rapidly and potently promotes mitochondrial function through STAT3, Cell Commun. Signal 14 (2016) 32.
[32] K. Banerjee, M.P. Keasey, V. Razskazovskiy, N.P. Visavadiya, C. Jia, T. Hagg, Reduced FAK-STAT3 signaling contributes to ER stress-induced mitochondrial dysfunction and death in endothelial cells, Cell. Signal. 36 (2017) 154–162.
[33] A. Pozzi, R. Zent, ZO-1 and ZONAB interact to regulate proximal tubular cell differentiation, J. Am. Soc. Nephrol. 21 (2010) 388–390.